한국측지학회지, 제 13 권, 제 2 호, pp.291~298(1995년 12월 30일)

Computations of Terrain Effect within a Limited Area in Geodetic Gravity Field Modelling

Yun, Hong-Sic* · Suh Yong-Woon**

ABSTRACT

This paper describes the test results of terrain corrections as the short wave length effect and geoid effects in gravity field modelling using Digital Terrain Model(DTM) in Korea. For a rigorous determination of terrain correction a dense grided DTM data wave prepard spacing 500×500 m was used for the computation of terrain effects. From the results obtained by the mass prism model and the mass line model, we were found that the terrain effects are large depend on the topography in the test area. It means that we should considered the terrain effects for the precise geoid determination.

要　　旨

본 연구에서는 중력장모델링에 있어서 단 파장의 효과인 지형보정량을 계산하고 지오이드의 효과에 미치는 DTM 데이타를 사용하여 계산하였다. 정밀한 지형보정량을 계산하기 위하여 500×500 m 격자 간격의 DTM 데이타를 준비하여 매스프리즘 모델과 매스라인모델을 적용하였다. 적용결과 지형효과가 다소 크게 나타났으며, 이 결과는 정밀한 지오이드의 계산을 위하여는 지형효과가 고려되어야 한다는 것을 알 수 있었다.

1.INTRODUCTION

The topography of the area, in which geoidal heights are required, can contribute significantly to the short wavelength/high frequency part of the gravity spectrum. The terrain corrections, which refer to the gravitational effects on the gravity anomaly due to upper crustal mass bodies, can be determined by considering various terrain effects. The topography in a mountainous area affects gravity field modelling in two ways[3]:

(1) A strong gravity signal is due to the gravitational attraction of the topographic masses itself, a signal which dominates at shorter wavelengths, and therefore information of topography can be used to smooth the gravity field prior to any modelling process.

*Lecturer, Department of Civil Engineering, Sung Kyun Kwan University

**PhD. student, Department of Civil Engineering, Sung Kyun Kwan University

(2) The topography implies that the basic observation data -notably gravity anomalies -are given on a non-level surface; violating the basic requirements for Stokes' integral.

In the first case the gravity field may be smoothed by terrain reductions, in the second case Molodensky or Helmert condensation corrections are applied to offset the non-level surface.

The objective of this paper is the computation of terrain effects based on a variety of data and, using different spectral techniques. The numerical experiments are carried out in the following test area: [Latitude:34°45'~36°15'; Longitude: 127°30'~129°45'].

Terrain effects are computed using the classical planar FFT formulas and the space-domain integration. The results obtained from the FFT method are compared with those obtained by the space-domain integration. The evaluation of accuracy refers to the difference of the terrain cor-

rections derived from FFT and space-domain integration.

2. MATHEMATICAL MODEL

2.1 The Rigorous Terrain Correction Formula

The terrain correction at a point(x_i, y_i) is

$$c(i,j) = -G\iiint_{E}^{h_{ij}} \frac{\rho(x,y,z)(h_{ij}-z)}{r^3(x_i-x,\, y_j-y,\, h_{ij}-z)}\, dxdydz \qquad (1)$$

where G is Newton's gravitational constant, $\rho(x,y,z)$ is the topographic density at the running point, h_{ij} is the topographic height at point (i,j), E denotes the integration area, r(x,y,z) is the distance kernel. The distance kernel is as follows:

$$r(x, y, z) = (x^2 + y^2 + z^2)^{1/2} \qquad (2)$$

Using a gridded digital terrain model and taking the density as constant, equation(1) can be written as

$$c(i,j) = -G\,\rho \sum_{N-1M-1}^{n=0m=0} \int_{x_n-\Delta x/2}^{x_n+\Delta x/2} \int_{y_n-\Delta y/2}^{y_n+\Delta y/2} \int_{h_n}^{h_{ij}} \left[\frac{(h_{ij}-z)}{r(x_i-x, y_i-y, h_{ij}-z)} \right] dxdydz \qquad (3)$$

or

$$c(i,j) = -G\,\rho \sum_{N-1M-1}^{n=0m=0} \int_{x_n-\Delta x/2}^{x_n+\Delta x/2} \int_{y_n-\Delta y/2}^{y_n+\Delta y/2} \left[\frac{1}{r(x_i-x, y_i-y, o} - \frac{1}{r(x_i-x, h_{ij}-h_{nm}} \right] dxdydz \qquad (4)$$

With different terrain representation, c(i,j) can be expressed in different forms.

In practical applications, the terrain is digitized on a regular grid. The height within each cell is represented by a prism with mean height and mean density of the terrain as shown in Figure 1(a),

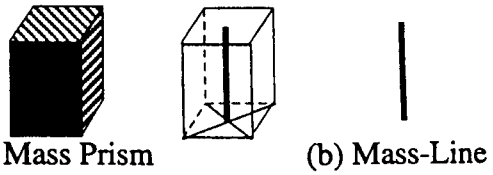

(a) Mass Prism (b) Mass-Line

Fig. 1. Two different topographic representations

which is called the mean prism terrain model. If the mass of the prism is mathematically concentrated along its vertical symmetric axis, then the terrain within the prism is represented by a line as shown in Figure 1(b), which gives the mass line terrain model. With the mass prism terrain model, assuming the mass within a prism is homogeneous and carrying out the double integration in equation (4), the expression for the terrain correction c(i,j)is obtained as

$$c(i,j) = -G\,\rho \sum_{n=0m=0}^{N-1M-1} [x\ln(y+r(x,y,z))) + y\ln(x,y,z)) - z\arctan\frac{xy}{zr(x,y,z)}] \begin{bmatrix} x_i-(x_n+\Delta x/2) & y_i-(y_n+\Delta y/2) & o \\ x_i-(x_n-\Delta x/2) & y_i-(y_n-\Delta y/2) & h_{ij}-h_{nm} \end{bmatrix} \qquad (5)$$

When the mass within a prism is concentrated along a line, instead of carrying out the double integration in equation(4), the terrain correction is simply expressed as

$$c(i,j) = -G\,\rho\,\Delta x\,\Delta y \sum_{n=0m=0}^{N-1M-1} \left[\frac{1}{r(x_i-x, y_i-y, o} - \frac{1}{r(x_i-x, h_{ij}-h_{nm}} \right] dxdydz$$

It is easy to understand that the mass line model is less realistic than the mass prism model from the physical point of view; therefore, it is worth investigating how big the effect on the terrain corrections will be when the mass line model is used instead of the mass prism model.

2.2 Computation of Terrain Correction via 2D FFT

2.2.1 Formulas with the mass line topographic model

With the mass line topographic model, the terms containing $1/r(x_i-x_n,\ y_j-y_m,\ 0)$ can be computed directly as will be seen later. The only thing we have to do is to express the terms containing $1/r(x_i-x_n,\ y_j-y_m,\ h_{ij}-h_{nm})$ as two-dimensional convolutions. Expanding $1/r(x_i-x_n,\ y_j-y_m,\ h_{ij}-h_{nm})$ in equation (4) into a Taylor series, the c(i,j) can be expressed as[14, 8, 9]

$$c(i,j)=co(i,j)+c1(i,j)+c2(i,j)+c3(i,j)+\cdots \tag{7}$$

where

$$c_0(i,j) = -G\rho\Delta x\Delta y\sum_{n=0}^{N-1}\sum_{m=0}^{M-1}\left[\frac{1}{r(x_i-x_n,y_i-y_m,o)}-\frac{1}{r(x_i-x_n,y_j-y_m,\alpha)}\right]dxdydz \tag{8}$$

$$c_k(i,j) = (-1)^{k+1}G\rho\Delta x\Delta y\frac{(2k-1)!!}{(2k)!!}\sum_{n=0}^{N-1}\sum_{m=0}^{M-1}\left[\frac{((h_{ij}-h_{nm})^2-\alpha^2)^k}{r^{2k+1}(x_i-x_n,y_i-y_m,\alpha)}\right] \tag{9}$$

$c_1(i,j)$ is the same expression as in Sideris (1984) for $\alpha=0$. The objective of adding the parameter α is to speed up the convergence of the series in equation (7). α was chosen as the average height in the computation area or the difference between the maximum and the minimum height.[1] From the mathematical point of view, the optimal value for α should be chosen as[9,15]

$$\alpha=\left[\frac{1}{NM}\sum_{N-1}^{n=0}\sum_{M-1}^{m=0}(\bar{h}-h_{nm})^2\right]^{1/2} = \sigma_h \tag{10}$$

i.e., the optimal value for α is the standard deviations of the heights.

Expanding the numerator of equation(9) into a series, ck(i,j) can be equivalently expressed as a set of two-dimensional convolutions to which the fast Fourier transform can be applied. The final expressions are

$$c_0(i,j) = G\rho F^{-1}\{H_oR_o\}, \tag{11}$$

$$c_1(i,j) = \frac{G\rho}{2}[(h_{ij}^2-\alpha^2)F^{-1}\{H_0R_0\} -2h_{ij}F^{-1}\{H_1R_1\}+F^{-1}\{H_2R_1\}], \tag{12}$$

$$c_2(i,j) = \frac{3G\rho}{8}[(h_{ij}^2-\alpha^2)^2F^{-1}\{H_0R_0\} -4h_{ij}(h_{ij}^2-\alpha^2)F^{-1}\{H_1R_2\}+(6h_{ij}^2-2\alpha^2)F^{-1}\{H_2R_2\} -4h_{ij}F^{-1}\{H_3R_2\}+F^{-1}\{H_4R_2\}], \tag{13}$$

$$c_3(i,j) = \frac{15G\rho}{48}[(h_{ij}^2-\alpha^2)^3F^{-1}\{H_0R_3\}-6h_{ij}(h_{ij}^2-\alpha^2)F^{-1} \{H_1R_3\}+3(h_{ij}^2-2\alpha^2)(5h_{ij}^2-2\alpha^2)F^{-1}\{H_2R_3\} -(20h_{ij}^2-12\alpha^2)h_{ij}F^{-1}\{H_3R_3\}+(15h_{ij}^2-3\alpha^2)F^{-1}\{H_4R_3\} -6h_{ij}F^{-1}\{H_5R_3\}+F^{-1}\{H_6R_3\}], \tag{14}$$

where

$$H_k=F\{h^k\},\ k=0,1,2,3,4,5,6 \tag{15}$$

$$R_o=F\left\{\Delta x\Delta\frac{y}{(x^2+y^2)^{1/2}}-\Delta x\Delta\frac{y}{(x^2+y^2+\alpha^2)^{1/2}}\right\};$$

$$R_k=F\left\{\Delta x\Delta\frac{y}{(x^2+y^2+\alpha^2)^{2k+1}}\right\},k=1,2,3,\quad \alpha=\sigma_h \tag{16}$$

Considering the fact that equation(8) represents the attraction of a mass layer with thickness α, $c_0(i,j)$ can be identically expressed as[9]

$$c_o(i,j)=Grho[(x\ln(y+r(x,y,z))+y\ln(x+r(x,y,z)))]\Big|_{z=\alpha}^{z=0} + \alpha\arctan\frac{xy}{\alpha r(x,y,\alpha)}]\Big|_{x=(1-i)\Delta x\ y=(1-j)\Delta y}^{x=(N-i)\Delta x\ y=(M-j)\Delta y} \tag{17}$$

For non-edge points, $c_0(i,j)$ can be approximated as the attraction of a mass cylinder with height α. When the radius of the cylinder tends to infinite, $c_0(i,j)$ can be simply evaluated by

$$co(i,j) = 2\pi G\rho\alpha \tag{18}$$

The conventional method to derive the two-dimensional convolutions is, first, to expand 1/r in equation (1) into series with respect to z, then to carry out the integration as done in Tziavos et al. (1988).

This procedure is equivalent to expanding both $1/\gamma(x_i-x_n,\ y_i-y_m,\ 0)$ and $1/\gamma(x_i-x_n,\ y_i-y_{m,\ hij}-h_{nm})$ into series. Consequently, the terrain correction c(i,j) is

$$c(i,j) = c_1(i,j)+c_2(i,j)+c_3(i,j)+\cdots \tag{19}$$

with

$$c_1(i,j) = \frac{G\rho}{2}[(h_{ij}^2F^{-1}\{H_0R_1\}-2h_{ij}F^{-1}\{H_1R_1\} +F^{-1}\{H_2R_1\}], \tag{20}$$

$$c_2(i,j) = \frac{3G\rho}{8}[((h_{ij}^2-\alpha^2)^2-\alpha^4)F^{-1}\{H_0R_2\} -4h_{ij}(h_{ij}^2-\alpha^{2)}F^{-1}\{H_1R_2\}+(6h_{ij}^2-\alpha^{2)F^{-1}}\{H_2R_2\} -4h_{ij}F^{-1}\{H_3R_2\}+F^{-1}\{H_4R_2\}], \tag{21}$$

$$c_3(i,j) = \frac{15G\rho}{48}[((h_{ij}^2-\alpha^2)^3--\alpha^6)F^{-1}\{H_0R_3\} -6h_{ij}(h_{ij}^2-\alpha^2)^2F^{-1}\{H_1R_3\}+3(h_{ij}^2-\alpha^2)(5h_{ij}^2-\alpha^2)F^{-1}\{H_2R_2\} -(20h_{ij}^2-12\alpha^2)h_{ij}F^{-1}\{H_3R_3\}+(15h_{ij}^2-3\alpha^2)F^{-1}\{H_4R_3\} -6h_{ij}F^{-1}\{H_5R_3\}+F^{-1}\{H_6R_3\}], \tag{22}$$

where H_k and R_k are the same as in equation(15) and (16). The optimal value for the parameter α in this case, however, should provide the smallest differences between $\gamma(x_i-x_n,\ y_i-y_{m,\ hij}-h_{nm})$ and $\gamma\ (x_i-x_n,\ y_i-y_m,\ \alpha)$ as well as between $\gamma\ (x_i-x_n,\ y_i-y_m,\ 0)$ and $\gamma\ (x_i-x_n,\ y_i-y_m,\ \alpha\ )$, which can be determined by minimizing the following variation function instead of equation(10):

$$J = \sum_{n=0}^{N-1}\sum_{m=0}^{M-1}\left((h_{ij}-h_{nm})^2-\alpha^2)^2+(0-\alpha^2)^2\right) \tag{23}$$

Correspondingly, the optimal value for α^2 is one-half of the variance of the heights, i.e.,

$$\alpha=\rho_h\sqrt{2} \tag{24}$$

2.2.2 Formulas with the mass prism topographic model

In equation(5), keeping the terms containing z=0 unchanged and expanding the terms containing $z=h_{ij}-h_{nm}$ into a series, the terrain correction formulas with the mass prism topographic model can be expressed as

$$c(i,j) = c_0(i,j)+c_1(i,j)+c_2(i,j)+c_3(i,j)+\cdots \tag{25}$$

where $c_0(i,j)$ can be evaluated directly according to equation(17) or (18). $c_1(i,j)$, $c_2(i,j)$ and $c_3(i,j)$ can be efficiently evaluated by means of the fast Fourier transform as

$$c_1(i,j) = \frac{G\rho}{2}[(h_{ij}^2-\alpha^2)F^{-1}\{H_0R_1\}-2h_{ij}F^{-1}\{H_1R_1\} +F^{-1}\{H_2R_1\}], \tag{26}$$

$$c_2(i,j) = \frac{G\rho}{8}[((h_{ij}^2-\alpha^2)^2-\alpha^4)F^{-1}\{H_0R_2\} -4h_{ij}(h_{ij}^2-\alpha^{2)}F^{-1}\{H_1R_2\}+(6h_{ij}^2-\alpha^{2)F^{-1}}\{H_2R_2\} -4h_{ij}F^{-1}\{H_3R_2\}+F^{-1}\{H_4R_2\}], \tag{27}$$

$$c_3(i,j) = \frac{G\rho}{48}[((h_{ij}^2-\alpha^2)^3-\alpha^2)F^{-1}\{H_0R_3\}-6h_{ij}(h_{ij}^2-\alpha^2)^2F^{-1} \{H_1R_3\}+3(h_{ij}^2-\alpha^2)F^{-1}\{H_2F_3\}(20h_{ij}^2-12\alpha^2)h_{ij}F^{-1} \{H_3R_3\}+(15h_{ij}^2-3\alpha^2)F\{H_4F_3\}-6h_{ij}F^{-1}\{H_5R_3\}+F^{-1} \{H_5R_3\}+F^{-1}\{H_6R_3\}], \tag{28}$$

where H_k is defined by equation (11) and

$$F_1 = F\ \{f_{11}(x,y,\alpha)+f_{11}(y,x,\alpha)-f_{12}(x,y,\alpha)\}, \tag{29}$$

$$F_2 = F\ \{f_{21}(x,y,\alpha)+f_{21}(y,x,\alpha)-f_{22}(x,y,\alpha)\}, \tag{30}$$

$$F_3 = F\ \{f_{31}(x,y,\alpha)+f_{31}(y,x,\alpha)-f_{32}(x,y,\alpha)\}, \tag{31}$$

$$\alpha= \sigma_h, \tag{32}$$

$$f_{11}(x,y,\alpha)=\frac{-x}{(y+r(x,y,\alpha)r(x,y,\alpha)}\begin{bmatrix} x_n+\Delta x/2 & y_m\Delta y/2 \\ x_n-\Delta x/2 & y_m\Delta y/2 \end{bmatrix} \tag{33}$$

$$f_{12}(x,y,\alpha)=\frac{xy(r^2+\alpha^2)}{(x^2y^2+\alpha^2r^2)r}-\frac{1}{\alpha}\arctan\frac{xy}{\alpha r}\begin{bmatrix}x_n+\Delta x/2 & y_m\Delta y/2\\ x_n-\Delta x/2 & y_m\Delta y/2\end{bmatrix} \quad (34)$$

$$f_{21}(x,y,\alpha)=\frac{-x(y+2r)}{3(y+r)^2r^3}\begin{bmatrix}x_n+\Delta x/2 & y_m\Delta y/2\\ x_n-\Delta x/2 & y_m\Delta y/2\end{bmatrix} \quad (35)$$

$$f_{21}(x,y,\alpha)=\frac{xy}{3(x^2y^2+\alpha^2r^2)r}\left[\frac{2(r^2+\alpha^2)^2}{x^2y^2+\alpha^2r^2}-\frac{r^2}{\alpha^2}+\frac{\alpha^2}{r^2}-4\right]-\frac{1}{3\alpha^3}\arctan\frac{xy}{\alpha r}\frac{xy}{\alpha r}\begin{bmatrix}x_n+\Delta x/2 & y_m\Delta y/2\\ x_n-\Delta x/2 & y_m\Delta y/2\end{bmatrix} \quad (36)$$

$$f_{31}(x,y,\alpha)=\frac{-x}{15(y+r)r^3}\left[\frac{1}{y+r}\left(\frac{y}{r^2}+\frac{4}{r}+\frac{2}{y+r}\right)+\frac{y}{r^2}\right]\begin{bmatrix}x_n+\Delta x/2 & y_m\Delta y/2\\ x_n-\Delta x/2 & y_m\Delta y/2\end{bmatrix} \quad (37)$$

$$f_{32}(x,y,\alpha)=\frac{xy}{15(x^2y^2+\alpha^2r^2)r}\left[\frac{3r^2}{\alpha^4}+\frac{6}{r^2}-\frac{3\alpha^2}{r^4}+\frac{2(r^2+\alpha^2)}{x^2y^2+\alpha^2r^2}+\frac{2(r^2+\alpha^2)}{x^2y^2+\alpha^2r^2}\left(11-\frac{2\alpha^2}{r^2}+\frac{r^2}{\alpha^2}-\frac{4(r^2+\alpha^2)^2}{x^2y^2+\alpha^2r^2}\right)\right] \quad (38)$$

Similarly, if the first term of $c_o(i,j)$ in equation(11) is also expanded into series, the following formulas can be derived:

$$c(i,j) = c_1(i,j) + c_2(i,j) + c_3(i,j) + \cdots \quad (39)$$

$$c_1(i,j)=\frac{G\rho}{2}[(h_{ij}^2-F^{-1}\{H_oF_1\}-2h_{ij}F^{-1}\{H_1R_1\}+F^{-1}\{H_2F_1\}], \quad (40)$$

$$c_2(i,j) = \frac{G\rho}{8}[((h_{ij}^2-\alpha^2)^2-\alpha^4)F^{-1}\{H_0R_2\} -4h_{ij}(h_{ij}^2-\alpha^2)F^{-1}\{H_1F_2\}+(6h_{ij}^2-\alpha^2)F^{-1}\{H_2F_2\} -4h_{ij}F^{-1}\{H_3R_2\}+F^{-1}\{H_4R_2\}], \quad (41)$$

$$c_3(i,j) = \frac{G\rho}{48}[((h_{ij}^2-\alpha^2)^3-\alpha^2)F^{-1}\{H_0F_3\}-6h_{ij}(h_{ij}^2-\alpha^2)^2F^{-1}\{H_1F_3\}+3(h_{ij}^2-\alpha^2)(5h_{ij}^2-\alpha^2)F^{-1}\{H_2F_3\}(20h_{ij}^2-12\alpha^2)h_{ij}F^{-1}\{H_3R_3\}+(15h_{ij}^2-3\alpha^2)F^{-1}\{H_4F_3\}-6h_{ij}F^{-1}\{H_5R_3\} +F^{-1}\{H_6R_3\}], \quad (42)$$

2.2.3 The unified terrain correction formulas via 2D FFT

The four sets of terrain correction formulas, namely equation(7) with equations(11) to (14), equation(19) to (22), equation(26) with equations (17), (26) to (28) and equations(39) to (42), can be uniformly expressed as

$$c(i,j) = \beta c_o(i,j)+c_1(i,j)+c_2(i,j)+c_3(i,j)+\cdots \quad (43)$$

with $c_o(i,j)$ is expressed as in equation (24),

$$c_1(i,j)=\frac{G\rho}{2}[(h_{ij}^2-\beta\alpha^2)F^{-1}\{H_oF_1\}-2h_{ij}F^{-1}\{H_1R_1\} +F^{-1}\{H_2F_1\}], \quad (44)$$

$$c_2(i,j) = \frac{G\rho}{8}[((h_{ij}^2-\alpha^2)^2-(1-\beta)\alpha^4)F^{-1}\{H_0K_2\} -4h_{ij}(h_{ij}^2-\alpha^2)F^{-1}\{H_1K_2\}+(6h_{ij}^2-2\alpha^2)F^{-1}\{H_2K_2\} -4h_{ij}F^{-1}\{H_3K_2\}+F^{-1}\{H_4K_2\}], \quad (45)$$

$$c_3(i,j) = \frac{G\rho}{48}[((h_{ij}^2-(1-\beta)\alpha^6)F^{-1}\{H_0F_3\}-6h_{ij}(h_{ij}^2-\alpha^2)^2F^{-1}\{H_1K_3\}+3(h_{ij}^2-\alpha^2)(5h_{ij}^2-\alpha^2)F^{-1}\{H_2K_3\}(20h_{ij}^2-12\alpha^2)h_{ij}F^{-1}\{H_3K_3\}+(15h_{ij}^2-3\alpha^2)F^{-1}\{H_4F_3\}-6h_{ij}F^{-1}\{H_6K_3\}], \quad (46)$$

where the parameter β is

$$\beta=\begin{cases}1, \text{ if } c_o(i,j) \text{ is computed directly}\\ 0, \text{ otherwise}\end{cases} \quad (47)$$

$K_i(i=1,2,3)$ is the Fourier transform of the kernel function defined by

K_i = R_i (equation(16) for the mass-line topographic model,
F_i (eqs.29,30,31) for the mass-prism topographic model, (48)

$H_i(i=1,2,3,4,5,6)$ is the Fourier transform of the height with power i, as expressed in equation(15). It is worth pointing out that all the above formulas are based on a flat-earth assumption.

3. THE PRACTICAL COMPUTATION OF TERRAIN EFFECTS

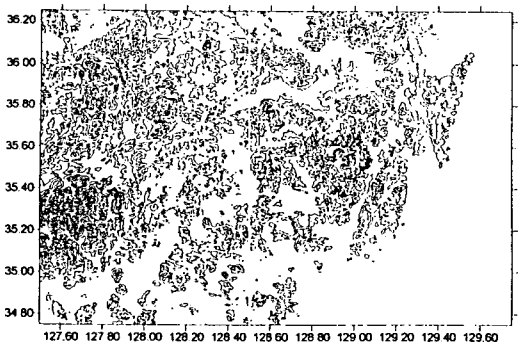

Fig. 2. Topography in the Pusan Area, Contour Interval: 500 m

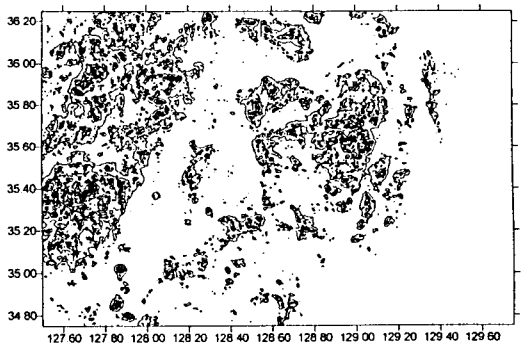

Fig. 3. Terrain corrections obtained from mass prism model. Contour Interval:2.5 mGal

Table 1. Statistics of topography in a test area

Max. Height	Min. Height	Mean Height	RMS	S.D.
1787.66 m	-0.5 m	182.68 m	296.25 m	233.22 m

Terrain corrections were computed on a 419 by 334 height grid in a test area in Pusan, bounded by latitude 34°45'N to 36°15'N and longitude 127°30'E to 129°45'E. The gridding interval is 500 m in each direction. Figure 2 shows the topography and the statistical information of the heights. The used DTM data were obtained from 1:50,000 topographic map by digitizing.

We were computed the topographic gravimetric corrections by means of the two dimensional fast Fourier transform and uses either mass prism topographic model or mass line topographic model. The formulas are expressed as a series of two-dimensional convolutions and the computation can be done up to the third term. Optimizations are made in to speed up the convergence of the series.

To investigate the effect of the difference representation of the topographic models, terrain corrections were computed with equation(5) and (6) by the numerical summation method. Equation(5) represents the mass prism (MP) topographic model, while (6) corresponds to the mass line(ML) model. The computations were done on a DEC 3000 with UNIX operating system.

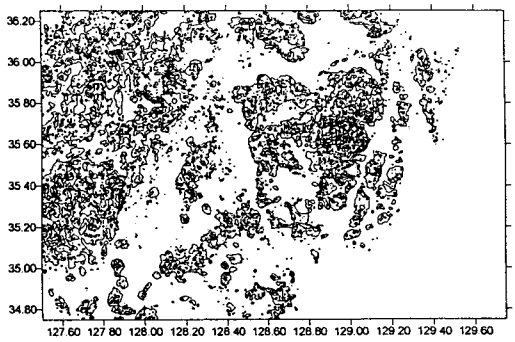

Fig. 4. The differences between mass-prism model and mass-line model. Contour Interval: 2.5 mGal

To show the effect of the different topographic representations, terrain corrections were computed at all the 419 by 334 points with a limited cap size of 100 km by 100 km. After zero-padding, the size of 2-D array is 818 by 668. The computation was done in the whole test area, with an integration cap size of 100 km by 100 km, and including the third-order term. The differences between the terrain corrections computed with the two different topographic models basically represent the errors due to the use of the mass line topographic model. Table 2 summarizes the statistics of both the terrain corrections and their contribution to the geoid undulation.

Figure 3 shows the terrain corrections obtained by mass prism mode and Figure 4 shows the differences of terrain corrections between two topographic models. Figure 5 shows the effect of the

Table 2. Effects of different models on terrain corrections and on geoid undulations

model	terrain correction(mGal)				effect on geoid prediction(m)			
	max.	min.	mean.	RMS	max.	min.	mean.	RMS
MP	31.26	0.00	1.66	1.44	0.112	-0.04	0.00	0.021
ML	29.65	0.00	1.514	1.33	0.101	-0.052	0.00	0.019
MP-ML	1.888	-0.002	0.144	0.127	0.005	-0.007	0.00	0.0025

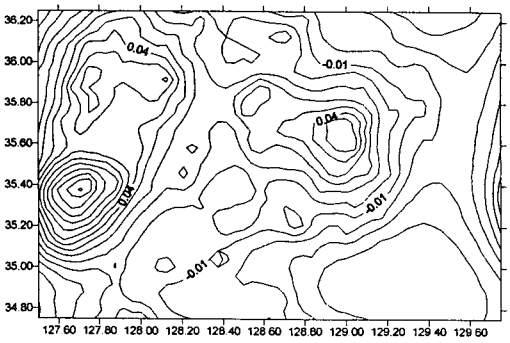

Fig. 5. The geoid undulations computed by mass-prism model. Contour Interval: 0.02 m

geoid undulations by mass prism model.

Table 2 indicates that the RMS of terrain correction error introduced the mass line topographic model is 0.13 mGal and the maximum value is 1.89 mGal. Comparing Figure 2 with Figure 3, it is obvious that the differences are correlated with the topography. The acquired effect of the geoid undulation is also the maximum value with 11 cm and minimum value with -4 cm. The RMS of obtained geoid undulation is 2 cm. Thus the conclusion is the same as that form equation(6); the rougher the topography is, the bigger the differences will be.

4. CONCLUSION

From the results obtained from this test computation, it is obvious that the terrain corrections are correlated with the topography. Thus, the rougher the topography is, the bigger the difference will be. Considering the acquired statistic values, we should be taken account the terrain effect for the precise geoid determination in Korea. This computation was done in a limited area because no more densed DTM data can be prepared. In this study we were compared between the mass-prism model and the mass-line model. Two models have not so big differences between each other. We may be applied these two models for the computation of the terrain effects in the geoid determination.

REFERENCE

1. Dorman, L. M. & Lewis, B.T.R., The use of nonlinear functional expressions in calculation of the terrain effect in airborne and marine gravimeter and geodimeter. Geophyics, 39. No.1, 1974, pp.33-38.
2. Ferland, R., Terrain corrections for gravity measurements. UCSE Rept. 20009, Division of Surveying Engineering. University of Calgary. Calgary, Alberta, Canada, 1984.
3. Forsberg, R., Terrain effects in geoid computation, Lecture Notes, International school for the determination and use of the geoid. Milano, Oct. 10-15, 1994.
4. Harrison, J.C. & Dickinson, M., Fourier transform method in local gravity field modelling. Bulletin Geodesique, 63, pp.149-166, 1989.
5. Haagmans, R., de Min, E. & van Gelderen, M., Fast evaluation of convolution integrals on the sphere using 1-D FFT, and a comparison with existing models for the Stokes' integral. Manuscripta Geodaetica, 18, pp.227-241, 1993.
6. Haaz, Z.B., Relations between the potential of attraction of the mass continued in a finite rectangular prism and its first and second deriatives(in Hungarian). Geofizikai Kozlemenyek, II, No.7, 1953.
7. Heiskanen, W.A. & Morits, H., Physcial Geodesy., W.

H. FreeMan and Company, SanFrancisco,1967.

8. Li. Y.C., Optimazed spectral geoid determination. UCSE Rept. 20050, Department of Geomatic Engineering, The University of Calgary, Canada, 1993.
9. Li, Y.C. & Sideris, M.G., Refined spectral terrain corrections for geoid determination, Presented at Scientific Meeting of Canadian Geophysical Union, Banff, AB, Canada, May 9-11, 1993.
10. Moritz, H., Local geoid determination in mountainous areas. OSU Rept. 353, Departement of Geodetic Science and Surveying, The Ohio State University, Ohio USA, 1983.
11. Schwaz, K.P., Data types and their spectral properties, Proceedings of Local Gravity Field Approximation. Beijing, China, Aug. 21- Sept., 1984.
12. Schwaz, K.P., Sideris M.G. & Forsberg, R., The use of FFT techniques in physical geodesy. Geophysics Journal 100, pp.485-514, 1990.
13. Sideris, M.G., Computation of the gravimetric terrain corrections using fast Fourier transform techniques. USCE Rept. 20007, Division of Surveying Engineering, University of Calgary, Alberta, Canada, 1984.
14. Sideris, M.G., Rigorous gravimetric terrain modelling using Molodensky's operator. Manuscripta Geodaetica, 15, pp. 97-106, 1990.
15. Tziavos, I.N., Sideris M.G., Forsberg N. & Schwaz, K. P., The effect of terrain on airborne gravity and gradiometry. J. Geophys. Res. 93. No. B8, pp. 9173-9186, 1988.